A Transfer Function Description of Sheet Metal Forming for Process Control

R. D. Webb*
Research Assistant.

D. E. Hardt
Associate Professor.

Laboratory for Manufacturing and Productivity,
Massachusetts Institute of Technology,
Cambridge, MA 02139

Three-dimensional forming of sheet metal parts is typically accomplished using one or two shaped tools (dies) that impart the necessary complex curvature and induce sufficient in-plane strain for part strength and shape stability. This research proposes a method of applying closed-loop process control concepts to sheet forming in a manner that automatically converges upon the appropriate tooling design. The problem of controlling complex deformation is reduced to a system identification problem where the die-part transformation is developed as a spatial frequency domain transfer function. This transfer function is simply the ratio of the measured change in spatial frequency content of the part and the die. It is then shown that such a transfer function can be used to implement closed-loop process control via rapid die redesign. Axisymmetric forming experiments are presented that establish the appropriateness of the linear transfer function description (via a test of superposition) and demonstrate the convergence properties of the proposed control method.

Introduction

Forming of three-dimensional sheet metal parts is one of the most efficient and material conservative methods of creating large complex shapes. It is used in both high volume (e.g., automobile) and low volume (e.g., airframes) production, but in both cases the cost of tooling development is dominant and often prevents use of this process for small lots of parts and for prototypes. Aside from expense, the time consuming process of fine-tuning a set of complex dies virtually eliminates sheet forming as a flexible manufacturing operation. One alternative is to create and store numerous die sets and implement rapid changeover systems. This alternative, however, does little to enhance design freedom, flexibility, or minimize the economic lot size, since the tooling must still be developed in the conventional manner. Thus, adaptation of sheet metal forming to effective small lot or prototype manufacturing will succeed only if the methods of designing and developing the tooling are simplified and automated.

Once it is acknowledged that the forming process is aimed at producing only in small lot sizes, it is clear that the robustness of the tooling must be relaxed in favor of reducing the cost and lead time of the tooling. A logical execution of this concept is to replace hardened, ground tooling with "soft" machined tooling. Beyond this, the ideal solution is to eliminate fixed tooling altogether, by using, for example, a die set of variable configuration. Such devices have been developed based on the concept of discrete forming surfaces, and a full scale, matched tooling draw press has been constructed as part of this research project [1], and is shown in Fig. 1. For tooling with nonsmooth surfaces, a neoprene interface between the tool and the part is a necessity, and the added compliance of the "tool" must be accounted for in the die design procedure.

Background

Forming of sheet metal can be accomplished in many ways, but the primary features of such deformation are general biaxial in-plane strain, combined with two-dimensional bending to produce net (often compound) curvature in the final part. A typical means for achieving such strains involves the use of matched dies plus a separate binder that is used to regulate the flow of material (in a draw forming operation) or to create a net stretching condition (in a stretch forming operation). (See Fig. 2.) While both die and binder design are relevant to production success, the latter is primarily concerned with regulating formability of the sheet by maintaining a strain state that avoids either an in-plane tensile or compressive instability condition. This stability problem has also been approached as a process control problem by Lee and Hardt [2], and Fenn and Hardt [3], but in this work it is treated separately from the shape control problem.

Assuming an appropriate binder condition, the process control task addressed here is to develop tooling shapes that will yield the correct part shape. The relationship between the die shape and the resulting part shape is a strong function of the elastic springback of the material, which in turn depends on both the loaded state of strain and the flow stress-strain properties of the workpiece. The complex geometries involved as well as the complex nature of sheet plasticity makes die design a formidable task.

*Now with The Timken Company, Canton, OH.

Contributed by the Production Engineering Division for publication in the JOURNAL OF ENGINEERING FOR INDUSTRY. Manuscript received April 1988; revised November 1989.

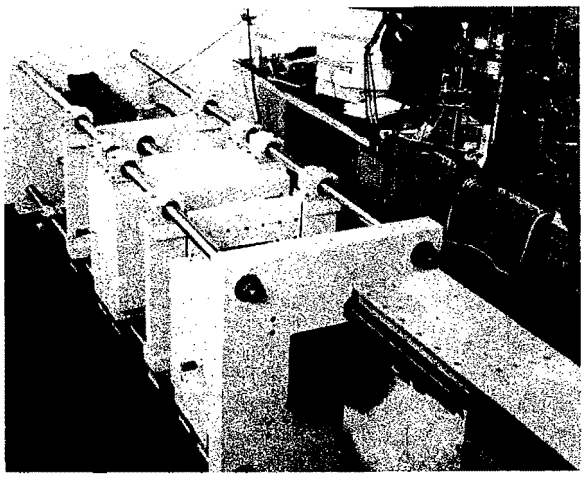

Fig. 1(a) Overall view of variable configurable die machine

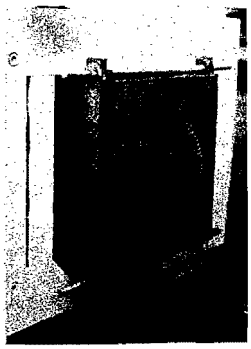

Fig. 1(b) Close-up of one die set

Fig. 1(c) Resulting part

Fig. 1 The MIT discrete die forming machine. The forming surface comprises a 12 in. × 12 in. bundle of 1/4 in. square elements, and the forming capacity is 60,000 lbs.

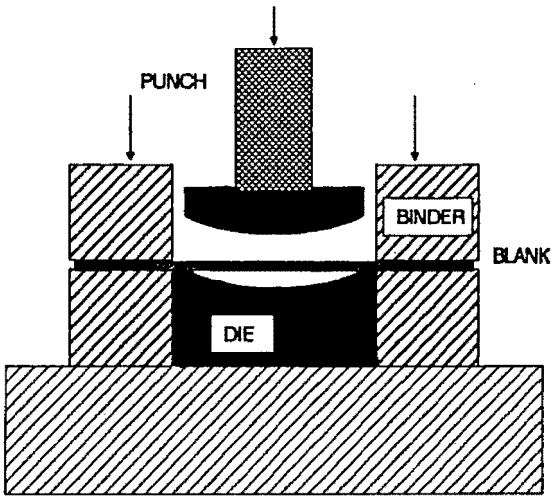

Fig. 2 A matched die forming operation

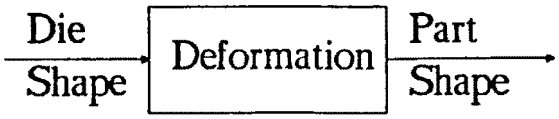

Fig. 3(a) A die-part block diagram model

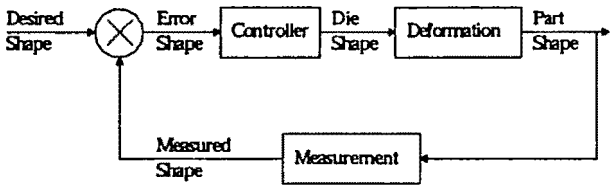

Fig. 3(b) A closed-loop sheet forming system

The approach taken here is to seek in-process measurements that reflect the forming result for a given die shape and to use part shape "errors" to correct the die shape in a consistent and predictable fashion (as opposed to purely heuristic iteration).

Complete in-process monitoring of deformation would require that the state of strain at all points in the sheet as well as the local stress-strain characteristics of the material be known throughout the process. This in turn mandates measurement of the three-dimensional strains (i.e., including thinning or thickening strains) as well as surface pressure and shear distributions. The impracticality of such an approach is clear, and it is equally important to realize that shape estimates based on strain measurements would be error prone, since they would require large scale spatial integration of potentially biased measurements.

Based on this simple observation, and on the overall goal of creating parts of the correct shape, the method adopted here uses the three-dimensional shape of the formed part as the key measurement for process control. Thus the process is now viewed as shown in Fig. 3(*a*), and the corresponding control problem is shown in Fig. 3(*b*).

The conventional alternative to this control approach is to seek a more analytical description of the process and to predict current tooling shapes based on process simulation. Because of the complex shapes involved, the strong dependence upon nonlinear material properties, and the complex interface geometries that occur during forming, this problem can only be attacked using numerical methods.

Major progress has been made recently in codes for large strain deformation [4] and in their application to complex forming [5]. However, there remain several severe limitations of this approach when considered for process control. Most prominent among these are the need for accurate constitutive relationships and the formidable computations required for parts of realistic geometric complexity. This recent history of Finite Element Analysis (FEA) in sheet forming is a chronology of progressively more complete material description with a concomitant penalty in computation time [5,6,7,8,9]. Also, the frictional characteristics of the die-workpiece and binder workpiece interactions have yet to be

carefully characterized [5, 10]. Finally, it must be understood that the objective of the work presented here and that of typical process analysis are in fact quite different. While process control seeks to answer the question "what tooling will produce the desired part?" FEA answers the inverse question: "what part will this tooling produce?" Such numerical models can be quite useful in understanding the details of a given deformation process, but their use in process control is limited by long computation time, and (more importantly), the noninvertability of the solution.

Control of forming based on in-process measurements has been demonstrated for several different forming methods. Stelson [11] has presented a method whereby in-process measurements are used to develop a material characterization in real-time that is then used to control a simple three point bending operation. Hardt et al. [12] have demonstrated the use of direct springback estimation from in-process measurements for simple roll bending, and further extended this to automatic straightening [13] and twisting [14]. The feature of these processes is that either elastic (springback) or extrinsic constitutive relationships (i.e., moment-curvature) can be estimated in-process. On the other hand, if no stress or moment information is available, it has been shown [15] that a springback estimate can be developed from a pair of successive deformation cycles and then used for process control.

Development of a Deformation Transfer Function (DTF)

Earlier work by the authors [16] has explored a very simple form of process control for three-dimensional shape control. The actual process control law changed the local die shape in response to local shape error regardless of any apparent coupling between adjacent points on the workpiece. While this rather blind iteration showed some amount of convergence in basic 3D forming experiments, it in fact lead to very poor process control accuracy. The present work seeks a means for process control that does not ignore the obviously highly coupled (or membrane-like) nature of sheet deformation, while at the same time obviates an excessively detailed mechanical analysis. To this end, it is important to consider the process control context of this research and how best to use the part shape measurements.

A typical description of three-dimensional surfaces comprises a set of Cartesian coordinates. It is useful to envision these as a collection of elevations (z coordinates) from a grid of equally spaced points (x, y coordinates). Thus a part or die shape is a matrix of elevations $\mathbf{z}(x, y)$ with respect to a reference plane. If we now use this description of shape in a part transformation description, we might look for simple differences between corresponding matrix elements for the desired part and the actual part and form an error matrix:

$$\mathbf{e}(x,y) = \mathbf{p}_{\text{des}}(x,y) - \mathbf{p}_{\text{actual}}(x,y) \tag{1}$$

If we then look at the corresponding matrix describing the die shape $\mathbf{d}(x,y)$, we can conceive of a control system that modulates this matrix in response to $\mathbf{e}$. A simple feedback control scheme would take the form:

$$\Delta\mathbf{d}(x,y) = \mathbf{g}(x,y)\mathbf{e}(x,y) \tag{2}$$

where $\Delta\mathbf{d}(x,y)$ is the change in the die shape and $\mathbf{g}(x,y)$ a controller matrix. The problem now is to design $\mathbf{g}$ to insure rapid convergence of the error to zero. Thus $\mathbf{g}$ is the embodiment of our knowledge about the forming process, and must adequately reflect the coupling between changes in part shape and die shape. Further, $\mathbf{g}$ should be continuously updated to reflect improved information about the current forming conditions and material properties.

However, as the forward has stated, we do not (and cannot) know enough about the forming process a priori to design $\mathbf{g}$ off-line, and also we know that using $\mathbf{g}=\mathbf{I}$ (the Identity matrix) leads to poor performance (as demonstrated in [16]). Thus we must have a method for discovering the best value for $\mathbf{g}$ *in-process*. To do so we can borrow from system identification concepts based on frequency response metods.

Before considering this method any further, however, it is first necessary to discuss alternative forms of using the shape information $\mathbf{z}(x, y)$. Left alone, shape change information based on this description carries no inherent coupling to the error equation (1) and does not reflect even a simple membrane model of forming. However, if the raw coordinates are replaced with some exact interpolating function (such as a polynomial function or spline curve), the coefficients of those functions can become the control variables. Since perturbing any one of the coefficients in these functions changes the corresponding curve everywhere, there is an inherent coupling effect that can be exploited in more accurate system modeling.

However, the choice of an interpolating function is critical to facilitating system identification and eventually process control. Accordingly, it was decided to use Discrete Fourier Transforms as the interpolating curves, since these would yield a spatial frequency domain description of the shape, which can then be used in a manner similar to temporal frequency domain information in conventional system identification and control methods.

The Discrete Fourier Transform for a given 2-D curve $y(n)$ (where n are discretized intervals in x) is given by:

$$\mathbf{Y}(m) = \sum_{n=0}^{N-1} y(n)e^{-j(2\,mn/N)};\ m=0,\ 1,\ \ldots\ N-1 \tag{3}$$

where $Y(m)$ is a complex array of magnitude and phase coefficients for the $N/2$ equally spaced frequencies from 0 to π/N. Likewise if we consider a three-dimensional shape $z(m, n)$, the corresponding transform is:

$$\mathbf{Z}(u,v) = \sum_{m=0}^{M-1}\sum_{n=-0}^{N-1} z(m,n)e^{-j2}[(mu/M) + (nv/N)]; \tag{4}$$

$$u=0,\ 1,\ \ldots,\ M-1$$
$$v=0,1,\ \ldots,\ N-1$$

where $\mathbf{Z}(u, v)$ is a matrix of complex (magnitude and phase) coefficients for the orthogonal discrete frequencies for 0 to π/M and 0 to π/N.

As with either polynomial or spline curve interpolators, the spatial frequency descriptor will carry with it inherent coupling from local coefficient changes to global shape changes. However, with shapes described by their spectral equivalent: $\mathbf{Z}(u, v)$, it is now possible to define the response of the forming process in terms similar to classic frequency response of dynamic systems.

Accordingly, the input-output transformation for the forming process shown in Fig. 3(a) can be defined as:

$$\mathbf{H}(u, v) = \frac{\mathbf{P}(u, v)}{\mathbf{D}(u, v)} \tag{5}$$

where $\mathbf{P}(u, v)$ and $\mathbf{D}(u, v)$ are the transforms of the corresponding part and die shapes, respectively.

Carrying the transfer function definition further, we can, by simply algebra, express the part shape spectrum as:

$$\mathbf{P}(u,v) = \mathbf{H}(u,v)\mathbf{D}(u,v) \tag{6}$$

This now illustrates the role of $\mathbf{H}$ as the current model of the deformation process. Thus we define $\mathbf{H}$ as the Deformation Transfer Function (DTF)

If $\mathbf{H}$ exists, it should also be possible to rewrite equation (6) as:

$$\mathbf{D}(u,v) = \mathbf{H}^{-1}(u,v)\mathbf{P}(u,v) \tag{7}$$

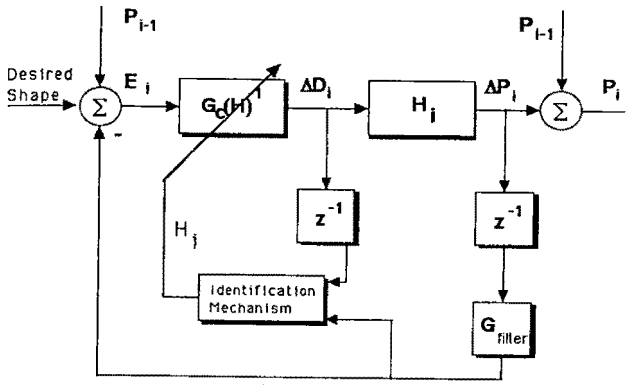

Fig. 4 Block diagram for a closed-loop system based on transfer function identification (z^{-1} indicates a delay of one forming cycle)

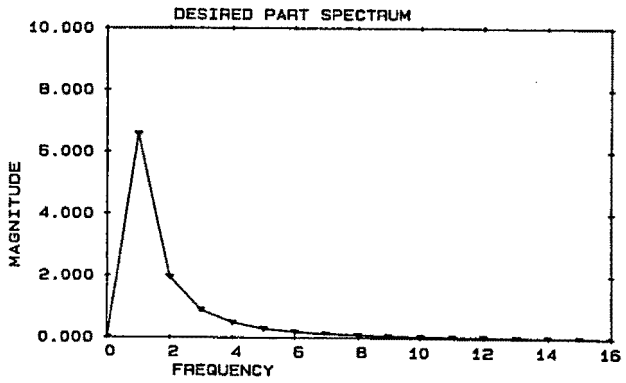

Fig. 5 Magnitude of the frequency components for the desired shape. (This is also the spectrum for the first tooling shape)

In doing so we have reached the goal of determining the die (**D**) that will produce the part **P**. Now all that remains is to:

(*1*) Develop a method to determine **H** in-process.

(*2*) Use the in-process determination of **H** to control the process of die shape design.

(*3*) Verify the validity of the DTF for 3-D sheet forming

In-Process Identification of the Deformation Transfer Function

If a part is formed using a particular die described by $\mathbf{D}_i$, and measurement of that part yields $\mathbf{P}_j$ (where the frequency arguments u and v are now assumed) then simple application of equation (5) would appear to have successfully determined $\mathbf{H}_i$. That is, the best estimate of the DTF is the current ratio of die and part spectra. However, the transfer function and attendant algebra is based on a linear model of deformation (or a linear model of the relaxation between the loaded shape of the part, given by $\mathbf{D}_i$, and the unloaded shape, given by $\mathbf{P}_i$). If equation (5) is treated as an absolute ratio, then it is in fact being used to describe a gross plastic deformation process.

Accordingly, the application of equation (5) must be confined to incremental changes in shape, and the DTF is to be redefined as:

$$\mathbf{H} = \frac{\Delta \mathbf{P}}{\Delta \mathbf{D}} \tag{8}$$

or in a form representative of successive forming trials:

$$\mathbf{H}_i = \frac{\mathbf{P}_i - \mathbf{P}_{i-1}}{\mathbf{D}_i - \mathbf{D}_{i-1}} \tag{9}$$

where i is a forming cycle index.

Thus, if two forming trials are performed using two different die shapes ($\mathbf{D}_i$ and $\mathbf{D}_{i-1}$), then the incremental DTF can be calculated.

As with any system identification, the choice of the "excitation" shape is critical to application of the DTF in a forming control situation. More will be said about this below, but in general it is necessary that all frequencies present in the desired shape be sufficiently excited in the identification steps to insure accurate representation in **H**. Also, the stationarity of **H** for forming is not guaranteed, thus continuous recalculation of **H** during a cycle of forming will be necessary.

Process Control Based on DTF Identification

Given the definition of the deformation Transfer Function **H** in equation (9), a method for closed-loop control of shape can be developed. If it is assumed that one calculation of **H** is sufficient to capture the process completely, then the following algorithm can be proposed:

Given $\mathbf{H}_i$:

$$\mathbf{D}_{i+1} = \mathbf{D}_i + \mathbf{E}_i \mathbf{H}_i^{-1} \tag{10}$$

where:

$$\mathbf{E}_i = \mathbf{P}_{\text{desired}} - \mathbf{P}_i$$

The implication is that the incremental DTF will give exactly the correct die correction based on the current discrepancy between the desired and actual part shape. A more general case would be where $\mathbf{H}^{-1}$ is used to determine the best control function $\mathbf{G}(\mathbf{H}^{-1})$ to insure rapid convergence when $\mathbf{H}^{-1}$ is not stationary.

Such a control system is illustrated in Fig. 4, where both the feedback of successive forming trials (separated by one cycle and represented by the delay function z^{-1}) and the in-process identification of $\mathbf{H}^{-1}$ is shown. (Notice also the allowance for a measurement filter $\mathbf{G}_f$ in the feedback loop.) In this form it takes on the character of self-tuning control, where the controller **G** is continuously updated according to the current best estimate of the process **H**.

A Two-Dimensional Test: Elastic-Plastic Bending

Given this definition of the DTF as a locally valid process description, the forming control algorithmm presented above can be explored. As a first test, the algorithm was applied in simulation to simple two-dimensional forming without stretching. This situation maximizes the elastic springback and serves to illustrate clearly the operation of the algorithm.

The desired shape was composed of a circular arc and two straight sections. Such a shape resembles a square pulse when plotted as curvature versus arc-length. This means that the curvature versus arc-length plots for the tooling profiles and their resulting part shapes will also resemble square pulses. Since the simulation calculates unloaded part shapes by numerically integrating curvature versus arc-length, the errors caused by numerical integration are small. The first shape is two straight sections joined by a single circular arc, while the second shape has three arcs. The first shape was described by:

$$y = -x - 1.75 \qquad -2.00 \le x \le -1.75$$

$$y = 1.75 - [2(1.75)^2 - x^2]^{1/2} \qquad -1.75 < x < 1.75$$

$$y = x - 1.75 \qquad 1.75 \le x \le 2.00$$

For this simulation, Young's modulus was 30×10^6 psi, the yield strength was 30×10^3 psi., and the shapes were represented by 32 equally spaced samples. Lacking a tolerance specification the algorithm was cycled five times.

In using this control algorithm, two precautions were taken to insure that $\mathbf{H}^{-1}$ was properly defined for each cycle. The first was to apply a low pass filter to the sampled data from both the tooling shapes and the part shapes. Since the system is acting off line, the filter consisted of simply not calculating

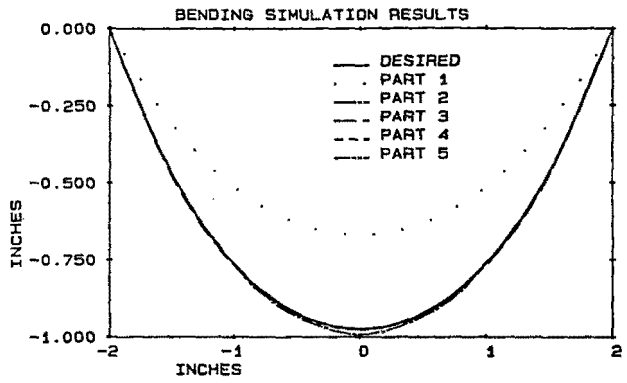

Fig. 6(a) Part shapes for five cycles of the control algorithm for 2D forming

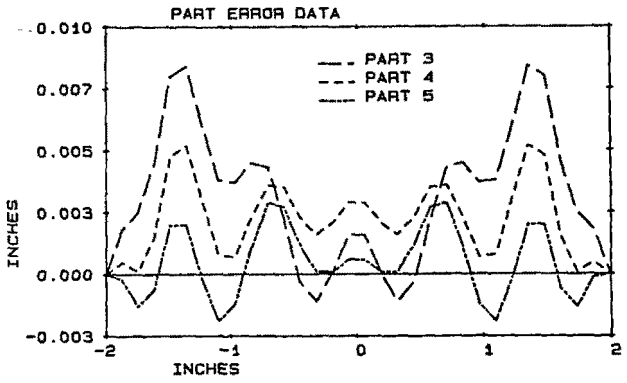

Fig. 6(b) Part shape error for the last three parts of (a)

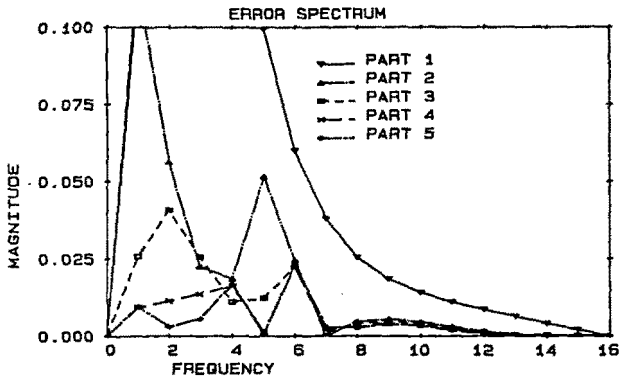

Fig. 6(c) Frequency spectrum of the part errors of (b)

Fig. 6 Results of 2D forming simulation

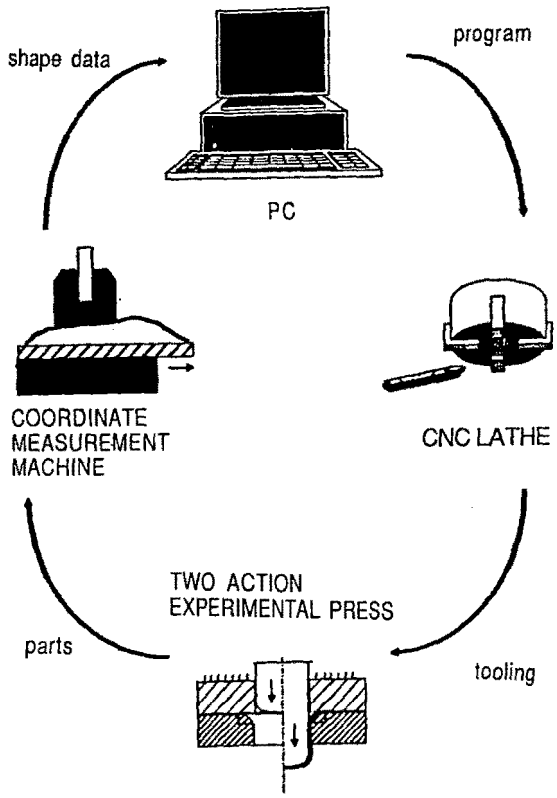

Fig. 7 Components of the axisymmetric forming system

$\mathbf{H}^{-1}$ above a predetermined cut-off frequency. The purpose of this filter is to avoid defining transfer function elements for those high frequency components that have insignificant magnitudes throughout the process. This cutoff frequency was chosen after observing the magnitude of the DFT of the desired part shape. In first case, after observing the spectrum of Fig. 5, the cut-off frequency was chosen as the seventh frequency component. The figure shows that the magnitudes of the frequency components above this cut-off are two orders of magnitude smaller than the magnitude of the fundamental frequency.

The second precaution was to define a threshold magnitude for the DFT of the change in part shape, $\mathbf{P}$. When the magnitude of a frequency component in $\mathbf{P}$ fell below the threshold, $\mathbf{H}^{-1}$ was considered undefined for that frequency and therefore set to zero magnitude. Recall that this threshold should reflect either the resolution of the part measurement system, or a spatial frequency based part tolerance specification. For this simulation the threshold was 0.006 in.

The simulation proceeded as follows:

Step 1 Sample the desired part shape; this shape is the first tooling profile.
Step 2 Fit the samples with cubic splines.
Step 3 Based on an elastic-plastic bending model find the loaded curvature and the arc-length.
Step 4 Calculate the springback curvature at each point and find the unloaded part curvature.
Step 5 Numerically solve the curvature-shape relationships using a forth order Runge-Kutta routine to get the unloaded part shape.
Step 6 Fit the part data with cubic splines.
Step 7 Sample spline fit to part as in step 1.
Step 8 Calculate part error.
Step 9 Use Discrete Fourier Transform on the part samples. Update $\Delta\mathbf{P}$,$\Delta\mathbf{D}$, and $\mathbf{E}_i$.
Step 10 Filter $\Delta\mathbf{P}_i$ so that $\mathbf{H}^{-1}{}_i$ is properly defined.
Step 11 Calculate $\mathbf{D}_{i+1}$ of new tooling shape using the control algorithm.
Step 12 Use the DTF on $\mathbf{D}_{i+1}$ to find the samples of the new tooling profile. Go to step 2.

The results of the simulation are shown in Fig. 6. It is clear from Fig. 6(*a*) that the algorithm quickly produces parts that are close to the correct shape. Under careful scrutiny, this figure shows that the part formed in forming cycle two overshot, i.e., it was over formed. This is not surprising since in this application of the algorithm, the first two "parts" are the flat blank (that will appear to be "formed" from flat tooling) and part one formed from tooling with the same shape as the desired shape.

Figure 6(*b*) shows the error between the desired part shape and the desired shape for the last three cycles. Note that the error in displacement has been confined to less than 0.005 in. for

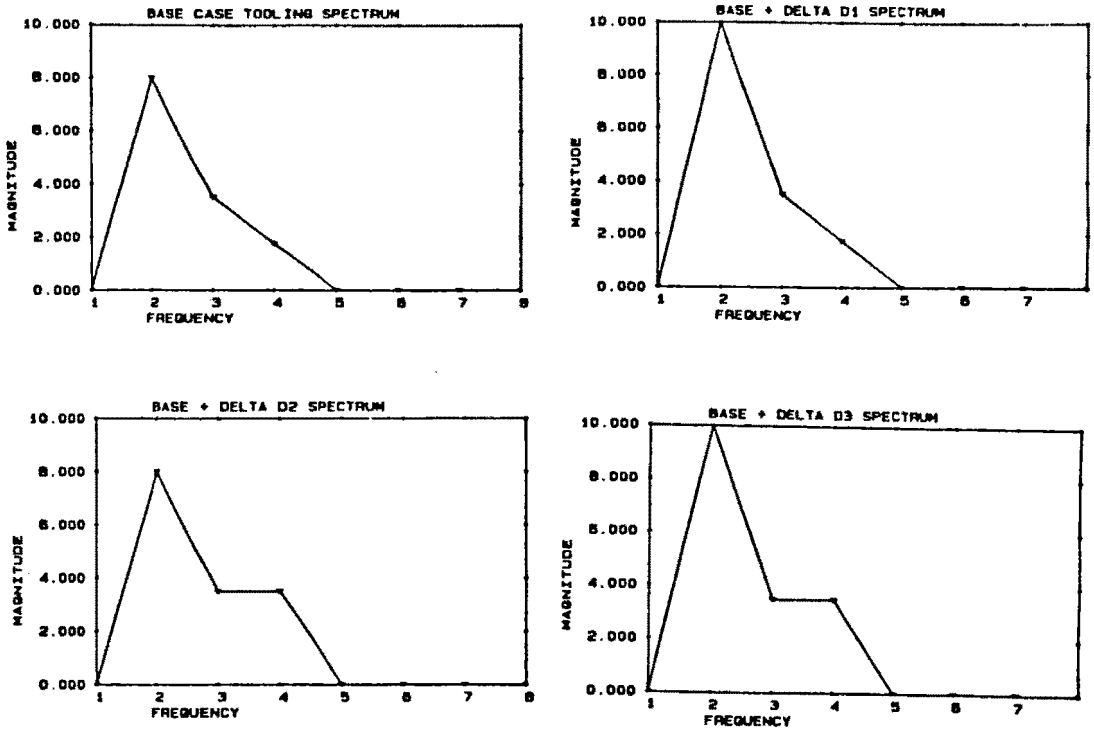

Fig. 8(a) Frequency spectrum for each shape

a part that has a maximum displacement of one inch, i.e., the error is less than 0.5 percent. This figure also suggests that the error remaining after five cycles consists of two superimposed sine waves.

This observation is supported by the magnitude of the frequency spectrum for the part errors shown in Fig. 6(*c*). Note that the magnitudes of the frequency components of the error in the last three forming cycles are below the magnitude threshold. This indicates that under the system limitations implied by the magnitude threshold, the closed loop forming system would have claimed success at the third part.

The conclusion here is that for the case of simple 2-D forming, the DTF based algorithm shows appropriate convergence. However, what remains is actual experiments in a 3-D forming condition. Accordingly, both the validity of the incremental DTF and the proposed algorithm are examined below in a series of axisymmetric forming experiments.

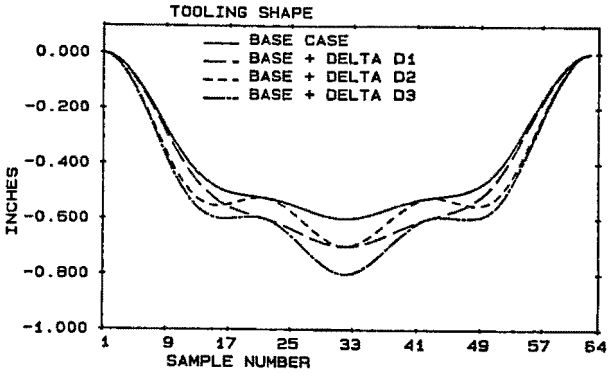

Fig. 8(b) Actual part shapes

Fig. 8 Four tooling shapes for the superposition trials

Experiments

Ideally the proposed DTF and associated control method would be tested in a general three-dimensional forming context. However, it is impractical at this time to produce and rapidly modify general 3-D tooling for forming (although a programmable tooling process has been developed, see [1] and [17], and is currently undergoing forming tests [18]). Consequently, a closed loop forming system was developed based on axisymmetric tooling that could be rapidly produced and modified using a CNC lathe. The system developed for this purpose is shown in Fig. 7, and in addition to the lathe, comprises a forming process capable of exact force control in both the binder and punch (see [2] for details) with a 4 in. diameter tooling capacity, a coordinate measurement machine (CMM), and a PC to control the overall loop. The PC controlled the CMM and used the resulting shape data to calculate new tooling profile. It then produced the necessary G-code for the lathe. Matched die sets were then machined and installed in the press, whereupon a part was formed. All experiments reported here also involved the use of 1/8 in. neoprene pads on either side of the material blank. (Forming trials without the pads were also executed as reported in [19].) Using this system, a complete tooling cycle took less than eight hours to complete.

For the experiments that follow, shapes were sampled 63 times along the part diameter of four in. For the part, the samples were taken parallel to the rolling direction of the sheet metal. The tooling shape is the shape of the path of the CNC cutting tool for the female (stationary) side of the tooling. The shape of the punches were generated by offsetting the die shape along the surface normal by the thickness of the sheet metal. Diametrically opposite samples were averaged, and the center point was then counted twice so that the Fast Fourier Transform (FFT) used to obtain the spectrum could operate upon 64 samples.

The material was 0.036 in. thick commercial quality steel. The initial diameter of the circular blanks was 5.75 in. The binder force was set at 1000 lbs., and the maximum punch force was set at 10,000 lbs. The difficulty of insuring registration between parts and tooling required that fresh blanks be used for each forming cycle.

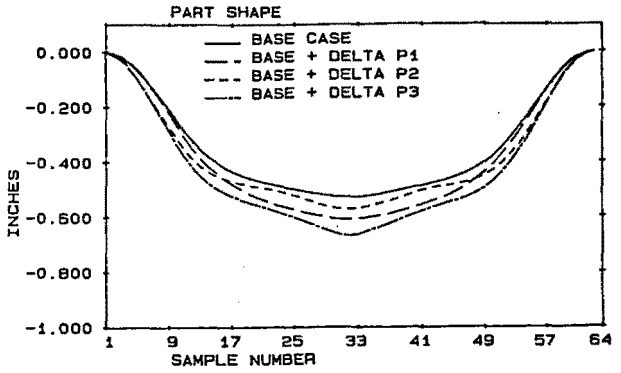

Fig. 9(a) The four parts generated by the tooling in Fig. 8

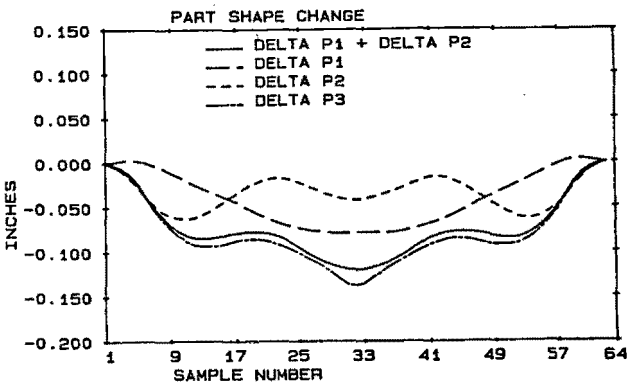

Fig. 9(b) Part shape change from (a)

Fig. 9 Results of superposition experiments

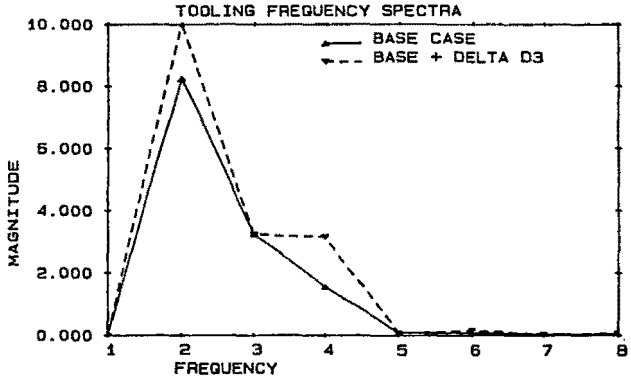

Fig. 10(a) Frequency spectrum of the tooling used to start the control algorithm

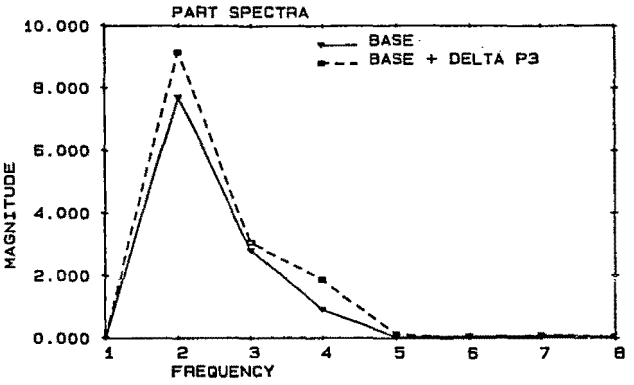

Fig. 10(b) Frequency spectrum of the parts formed using the tooling of Fig. 8

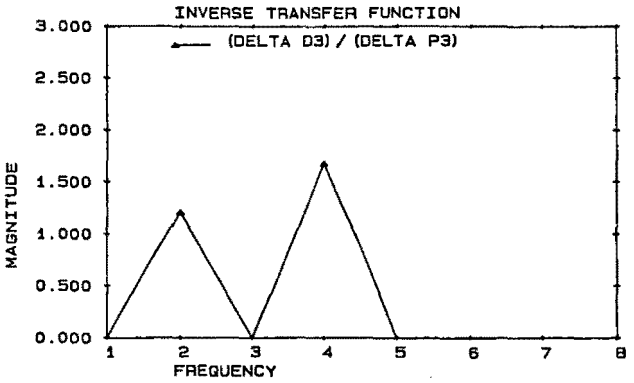

Fig. 10(c) Magnitude of H^{-1} calculated from (a) and (b)

Testing the Deformation Transfer Function: Superposition. The first tests were used to examine the basic response of the material in terms of the DTF method. In particular, the linearity of the process when viewed in the spatial frequency domain is of interest. All linear systems exhibit the property of superposition, i.e., the response to a combination of inputs is the same as the sum of responses to individual components of the input. In the case of forming, we can test for this property in the following way.

Given a (base case) tooling shape $\mathbf{D}$ that generates the part $\mathbf{P}$, suppose that two different tooling shapes $\mathbf{D}+\Delta\mathbf{D}_1$ and $\mathbf{D}+\Delta\mathbf{D}_2$ produce part shapes $\mathbf{P}+\Delta\mathbf{P}_1$ and $\mathbf{P}+\Delta\mathbf{P}_2$, respectively. If the deformation transfer function, $\mathbf{H}$, is linear, then the principle of super-position demands that if a third shape is defined as:

$$\Delta\mathbf{D}_3 = \Delta\mathbf{D}_1 + \Delta\mathbf{D}_2 \tag{11}$$

then

$$\Delta\mathbf{P}_3 = \Delta\mathbf{P}_1 + \Delta\mathbf{P}_2 \tag{12}$$

or that

$$(\Delta\mathbf{D}_1 + \Delta\mathbf{D}_2)\mathbf{H} = (\Delta\mathbf{D}_1)\mathbf{H} + (\Delta\mathbf{D}_2)\mathbf{H} \tag{13}$$

that is, the third shape can be described either by the sum of individual deformation trials, or a single "combined shape" trial.

For this experiment, the four tooling shapes were described by

Base:

$$z_{\text{base}} = -0.25\cos(r\omega) - 0.10\cos(2r\omega) - 0.05\cos(3r\omega)\ \text{in.} \tag{14}$$

Base + $\Delta\mathbf{D}_1$:

$$z_1 = -0.30\cos(r\omega) - 0.10\cos(2r\omega) - 0.05\cos(3r\omega)\ \text{in.} \tag{15}$$

Base + $\Delta\mathbf{D}_2$:

$$z_2 = -0.25\cos(r\omega) - 0.10\cos(2r\omega) - 0.10\cos(3r\omega)\ \text{in.} \tag{16}$$

Base + $\Delta\mathbf{D}_3$:

$$z_3 = -0.30\cos(r\omega) - 0.10\cos(2r\omega) - 0.10\cos(3r\omega)\ \text{in.} \tag{17}$$

for $0 \le r \le 2$(in.), $\omega = \pi/2$ radians/in.

Note that relative to the base tooling shape, the first tooling shape change is confined to the $\pi/2$ radians/in. frequency, while the second tooling shape change is confined to the $3\pi/2$ radians/in. frequency. The third tooling shape change combines the first and second changes. The four tooling shapes and their corresponding frequency contents are shown in Fig. 8.

The part shapes resulting from these tooling shapes are plotted in Fig. 9(*a*). This figure shows that the neoprene pads have heightened the differences between part shapes and tooling shapes, and attenuated the higher frequency components

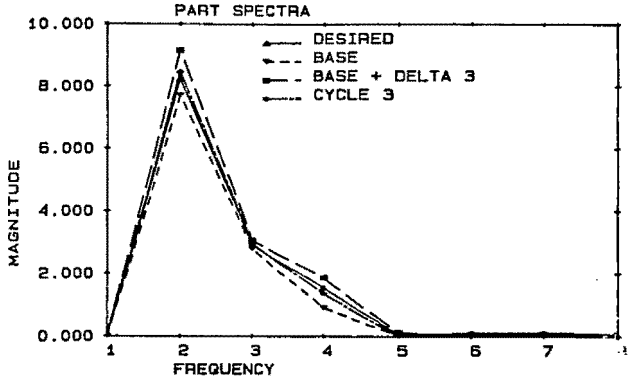

Fig. 11(*a*) Frequency spectrum for the parts formed

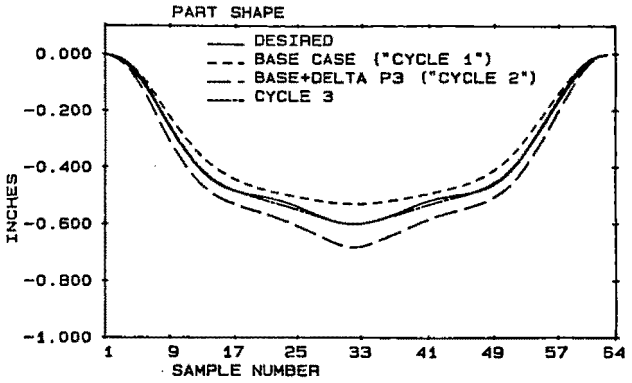

Fig. 11(*b*) Parts of (*a*) in spatial domain

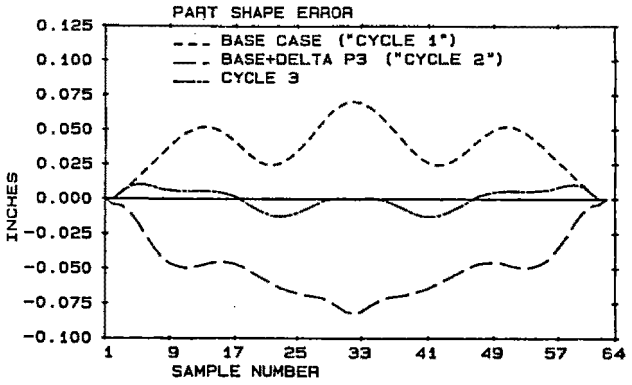

Fig. 11(*c*) Part shape errors from (*b*)

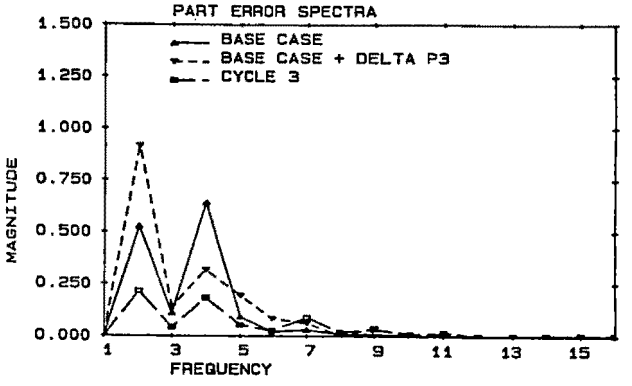

Fig. 11(*d*) Frequency content of errors in (*c*)

of the part shapes. Figure 9(*b*) plots the part shape differences from the base part shape. If the mechanics of part shape changes caused by tooling shape changes were exactly

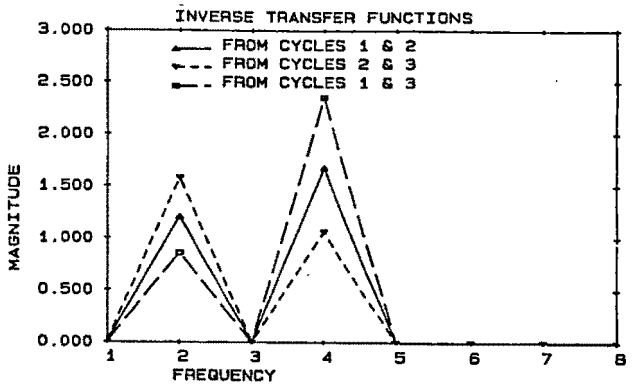

Fig. 12 Magnitudes of the H^{-1} DTFs generated by each forming cycle

linear, then the $\Delta\mathbf{P}_3$ curve would lie on top of the $\Delta\mathbf{P}_1 + \Delta\mathbf{P}_2$ curve. The shape difference between these two curves shows that, in this case, the neoprene pads have decreased the radius of curvature in the center of the $\Delta\mathbf{P}_3$ part. This would show up in the frequency domain as a small magnitude high frequency component. Overall, however, the curves are in good agreement. This observation supports the linear transfer function model of shape change that is central to the proposed control method.

Process Control Based on DTF Identification. Given this positive result, the control algorithm based on DTF identification can be explored. In [19] it was shown (both analytically and with axisymmetric experiments) that the initial tooling shape change used to start the algorithm must be sufficiently rich in spatial frequency content so that the first $\mathbf{H}^{-1}$ can be defined for all of the important frequency components in the desired part shape. The data from the superposition experiments described above is ideally suited to investigate this conclusion since it involves different shapes generated by different magnitudes of the same frequencies.

For the following experiment, "Cycle 1" was assigned to the base case (tooling $\mathbf{D}$, and part $\mathbf{P}$) of the super-position experiments. "Cycle 2" was assigned to the last case (tooling $\mathbf{D} + \Delta\mathbf{D}_3$, and part $\mathbf{P} + \Delta\mathbf{P}_3$) of the super-position experiments. Comparing the frequency spectra of the two tooling shapes, Fig. 10(*a*), and the frequency spectra of the two resulting part shapes, Fig. 10(*b*) reveals that the shape changes for the two cycles are confined to two frequencies. This means that the inverse transfer function identified by the algorithm is also confined to the same two frequencies, see Fig. 10(*c*). The implication here is that the algorithm should be able to correctly predict the tooling shape for any part shape that is different from the shape of the part shape of Cycle 1 (the base case) at only these two frequencies.

To test this assertion, a desired part shape was chosen that is different from Cycle 1 at only these two frequencies. A new forming trial, Cycle 3, was performed with the tooling shape that the algorithm predicted would form this desired part shape, based upon the shape change data from Cycles 1 and 2. Figure 11(*a*) shows frequency spectra comparisons of the desired part shape and the part shapes of Cycles 1 through 3. This figure shows that each of these part shapes is confined to the same frequency components, and that the frequency spectra of these shapes are similar to each other. This similarity does not transform to the spatial domain, however. Figure 11(*b*) compares these same part shapes in the spatial domain.

The most striking feature of this plot is that while the part shapes of Cycles 1 and 2 do not strongly resemble the desired part shape, the third part shape is an excellent reproduction of that desired shape. This observation is reinforced in Fig. 11(*c*) that shows the part shape error for these three forming cycles.

Figure 11(d) shows the frequency spectra for these part shape errors. There are three interesting aspects of this figure. The first aspect to note is that Cycle 2 (part $\mathbf{P}+\Delta\mathbf{P}_3$) does have a high frequency error as suggested for the 2-D case. The second aspect of note is that in spite of this, the shape error for the three forming cycles are primarily described by the same two frequencies in the inverse transfer function in Fig. 11(a). The final aspect to note is that the algorithm has generated essentially the desired part shape for Cycle 3.

The fact that the part shape of Cycle 3 is not exactly the desired part shape highlights the nonlinear nature of the shape change process. Figure 12 shows that the inverse transfer function is not stationary, but changes depending upon which two of these forming cycles are considered. The implication here is that the inverse transfer function identified by considering Cycles 2 and 3 would cause the algorithm to continue to improve part shape resolution. It is not unreasonable to expect that the algorithm would need more forming trials to converge upon a part shape with tighter tolerances.

Discussion

The results from the analysis of the three dimensional forming data and from the axisymmetric experiments show that under the proper conditions, the process of changing part shapes by changing tooling shapes can be modeled by a linear shape change transfer function acting upon spatial frequencies. Basically, the proper conditions consist of keeping the shape changes small, while insuring that these changes excite all of the important spatial frequencies. When these conditions are satisfied, this linear transfer function can be identified from forming trials on two different tooling shapes. The axisymmetric superposition experiments with neoprene show that this concept is valid even when there might be significant absolute shape differences between the tooling shapes and the resulting part shapes.

As a consequence of the conclusions concerning the validity of the shape change transfer function concept, it is not surprising that the algorithm based upon identifying these transfer functions is successful. As would be expected, the algorithm performs best when the conditions are ideal for linearly modeling the tooling-shape-change-part-shape-change interaction. The first shape considered in the bending simulations and the last axisymmetric experiment with neoprene show that the algorithm is capable of generating essentially the proper die shape for the third forming trial. Axisymmetric experiments that were performed without neoprene [19] showed similar rapid convergence for those frequencies for which the transfer function could be properly defined.

Conclusions

The Deformation Transfer Function method is intended to be applied to process control. It makes no attempt to actually model the physical process of deformation, rather, it provides a means for rapid in-process modeling of the local deformation recover process so as to aid in rapid die redesign. In one sense it is a new language for tooling and part shape description in the context of process operation.

Future work on this concept will concentrate on methods for control system compensator design that will allow more rapid convergence (most probably through attacking the high frequency errors that tend to remain after several forming trials) and on extending the experiments to the general three-dimensional case. The authors [20] have developed the general 3-D equivalent of the DTF method and shown its applicability to actual formed 3-D parts, but it has not yet been tested for general 3D forming trials.

It is expected that the method will find eventual application to both conventional die design, where tooling is designed using a combination of FEA and the proposed control algorithm, and to Flexible Forming Systems (FFS) where novel machines with rapidly reconfigurable tooling will replace conventional presses and permit economical one-of-a-kind part production.

Acknowledgments

This work was supported primarily by the National Science Foundation Grant no. 8214087-MEA with additional support from The Timken Company, General Motors, and ALCOA.

References

1 Robinson, R. E., "Design of an Automated Variable Configuration Die and Press for Sheet Metal Forming," S.M. Thesis, Department of Mechanical Engineering, M.I.T., Feb., 1987.

2 Lee, C. Y. G., and Hardt, D. E., "Closed-Loop Control of Sheet Metal Stability During Stamping," *13th North American Manufacturing Research Proceedings*, May 1985.

3 Fenn, R., and Hardt, D. E., "Real-Time Sheet Forming Stability Control," *Proceedings of the International Deep Draw Research Group*, June, 1990.

4 Arlinghaus, F. J., Frey, W. H., Stoughton, T. B., and Murphy, B. K., "Finite Element Modeling of a Stretch-Formed Part," *Proceedings of the American Institute of Mining, Metallurgical, and Petroleum Engineers*, April 29, 1985.

5 Chandra, A., "A Generalized Finite Element Analysis of Sheet Metal Forming with an Elastic-Viscoplastic Material Model," ASME JOURNAL OF ENGINEERING FOR INDUSTRY, Jan. 86.

6 Wang, N. M., and Budiansky, B., "Analysis of Sheet Metal Stamping by a Finite Element Method," ASME *Journal of Applied Mechanics*, Vol. 45, 1978.

7 Wang, N. M., and Wenner, M. L., "Elastic-Viscoplastic Analysis of Simple Stretch Forming Problems," *Mechanics of Sheet Metal Forming*, Koistinen, D. P., ed, Plenum Press, 1978.

8 Wang, N. M., "A Rigid-Plastic Rate-Sensitive Finite Element Method for Modeling Sheet Metal Forming," *Numerical Analysis of Forming Processes*, Pittman, J. F. T., Zienkiewicz, O. C., Wood, R. D., and Alexander, J. M., eds., John Wiley & Sons, 1984.

9 Kobayashi, S., and Kim, J. H., "Deformation Analysis of Axisymmetric Sheet Metal Forming Processes by the Rigid-Plastic Finite Element Method," *Mechanics of Sheet Metal Forming, Material Behavior, and Deformation Analysis*, Koistinen and Wang, eds., Plenum Press, 1978.

10 Wilson, W. R. D., "Friction and Lubrication in Sheet Metal Forming," *Mechanics of Sheet Metal Forming, Material Behavior, and Deformation Analysis*, Koistinen and Wang, eds., Plenum Press, 1978.

11 Stelson, K. A., and Gossard, D. C., "An Adaptive Pressbrake Control Using an Elastic-Plastic Material Model," ASME JOURNAL OF ENGINEERING FOR INDUSTRY, Vol. 104, Nov. 1982, pp. 289–293.

12 Hardt, D. E., Roberts, M. A., and Stelson, K. A., "Material Adaptive Control of Sheet Metal Roll Bending," ASME *Journal of Dynamic System, Measurement, and Control*, Vol. 104, No. 4, 1982.

13 Hardt, D. E., and Hale, M., "Closed-Loop Control of a Roll-Straightening Process," *Annals of CIRP*, Vol. 33, 1984.

14 Hardt, D. E., Jenne, T., Domroese, M., and Farra, R., "Real-Time Control of Twist Deformation Processes," *Annals of CIRP*, 1987.

15 Hardt, D. E., and Chen, B. S., "Control of a Sequential Brakeforming Process," ASME JOURNAL OF ENGINEERING FOR INDUSTRY, Vol. 107, May 1985.

16 Hardt, D. E., and Webb, R. D., "Sheet Metal Die Forming Using Closed-Loop Shape Control," *Annals of CIRP*, 1982.

17 Hardt, D. E., Webb, R. D., and Robinson, R. E., "Closed-Loop Control of Three Dimensional Sheet Forming," *Proceedings of the Eleventh NSF Conference on Production Research and Technology*, May 1984.

18 Knapke, J., "Forming with a Variable Configuration Die," S. M., Sept, 1988.

19 Webb, R. D., "Spatial Frequency Based Closed-Loop Control of Sheet Metal Forming," Ph.D. Thesis, M.I.T., May, 1987.

20 Webb, R. D., and Hardt, D. E., "Spatial Frequency Based Closed-Loop Control of a Sheet Forming Process," *Sensing and Control of Manufacturing Processes and Robots*, ASME Special Publication, Nov., 1984.